

## A facile approach to spinning multifunctional conductive elastomer fibres with nanocarbon fillers

This content has been downloaded from IOPscience. Please scroll down to see the full text.

2016 Smart Mater. Struct. 25 035015

(<http://iopscience.iop.org/0964-1726/25/3/035015>)

View [the table of contents for this issue](#), or go to the [journal homepage](#) for more

Download details:

IP Address: 194.27.18.18

This content was downloaded on 22/03/2016 at 10:53

Please note that [terms and conditions apply](#).

# A facile approach to spinning multifunctional conductive elastomer fibres with nanocarbon fillers

Shayan Seyedin<sup>1,2</sup>, Joselito M Razal<sup>1,2</sup>, Peter C Innis<sup>1</sup> and Gordon G Wallace<sup>1</sup>

<sup>1</sup>Intelligent Polymer Research Institute, ARC Centre of Excellence for Electromaterials Science, AIIM Facility, Innovation Campus, University of Wollongong, Wollongong, NSW 2522, Australia

<sup>2</sup>Deakin University, Geelong, VIC 3220, Institute for Frontier Materials, Australia

E-mail: [joselito.razal@deakin.edu.au](mailto:joselito.razal@deakin.edu.au) and [gwallace@uow.edu.au](mailto:gwallace@uow.edu.au)

Received 25 October 2015, revised 11 January 2016

Accepted for publication 27 January 2016


Published 22 February 2016



CrossMark

## Abstract

Electrically conductive elastomeric fibres prepared using a wet-spinning process are promising materials for intelligent textiles, in particular as a strain sensing component of the fabric. However, these fibres, when reinforced with conducting fillers, typically result in a compromise between mechanical and electrical properties and, ultimately, in the strain sensing functionality. Here we investigate the wet-spinning of polyurethane (PU) fibres with a range of conducting fillers such as carbon black (CB), single-walled carbon nanotubes (SWCNTs), and chemically converted graphene. We show that the electrical and mechanical properties of the composite fibres were strongly dependent on the aspect ratio of the filler and the interaction between the filler and the elastomer. The high aspect ratio SWCNT filler resulted in fibres with the highest electrical properties and reinforcement, while the fibres produced from the low aspect ratio CB had the highest stretchability. Furthermore, PU/SWCNT fibres presented the largest sensing range (up to 60% applied strain) and the most consistent and stable cyclic sensing behaviour. This work provides an understanding of the important factors that influence the production of conductive elastomer fibres by wet-spinning, which can be woven or knitted into textiles for the development of wearable strain sensors.

 Online supplementary data available from [stacks.iop.org/SMS/25/035015/mmedia](http://stacks.iop.org/SMS/25/035015/mmedia)

Keywords: composite fibres, fibre spinning, conductive elastomer, multifunctional materials, nanocarbons

(Some figures may appear in colour only in the online journal)

## 1. Introduction

It has been established that the addition of a filler to polymer matrices can impart useful functionalities such as enhanced mechanical properties and electrical conductivity [1–4]. A wide range of polymer composite materials have been produced and have found applications in flexible and stretchable electronics [5, 6], stretchable energy storage and conversion devices [7], sensors and actuators [8, 9], strain sensing [10–19], and electromagnetic interference

shielding [20]. Of technological importance are composites with strain sensing functionality. The homogeneity of conductive fillers in the elastomer matrix dictates the strain sensing property (i.e. the change in electrical resistance from an applied strain). Elastomers such as natural rubber [17], polyurethane (PU) [10, 13, 15, 18], and poly(styrene-*b*-isobutylene-*b*-styrene) (SIBS) [12, 14], and organic conductors such as polyaniline [15], polypyrrole [21, 22], poly(3-hexylthiophene) (P3HT) [14], poly(3,4-ethylenedioxythiophene):poly(styrenesulfonate) (PEDOT:

PSS) [18, 19], PEDOT:*p*-tosylate [10], carbon black (CB) [11], single-walled carbon nanotubes (SWCNT) and multi-walled carbon nanotubes [12, 13], and graphene [16] have been used previously for the production of conductive elastomer composites.

Recently, there has been a surge of interest in wearable strain sensors for application in body movement measurement [11, 23, 24], medical monitoring [25, 26], sports rehabilitation, and injury prevention [22, 27]. The development of wearable strain sensors requires fibres that are soft, and flexible, and that can preserve the inherent properties of textiles such as wearability and comfort; properties not realized with conventional silicon or metal-based electronics. However, the production of fibres with strain sensing functionality has been challenging because the addition of a conductive filler into an elastomer significantly affects the processability of the resultant formulations, in particular when using the fibre wet-spinning process, which is highly dependent upon the homogeneity of the spinning formulation.

Conductive elastomeric composite fibres need to possess critical properties to be used as functional strain sensors. They should be able to stretch and recover without significant deterioration in mechanical and electrical properties, because they will undergo cyclic deformation and relaxation during practical applications [14]. It is also important that these fibres can be made into a textile and/or incorporated within conventional fabrics by textile processing techniques such as knitting or weaving in order to realize the development of wearable strain sensors.

Achieving spinnability from composite formulations of elastomers and conductive fillers requires that the formulations are homogeneous (i.e. free from large aggregates) even at high filler loadings. This is difficult to achieve because most conducting fillers are inherently difficult to disperse in solvents and can also have poor compatibility with the elastomers. To date, there has been some success in spinning fibres from SIBS/P3HT [14], SIBS/SWCNT [12], and PU/PEDOT:PSS [18] with the resultant fibres displaying useful strain sensing properties. However, there is a lack of detailed understanding of how conductive fillers and their amount influence the electrical, mechanical, and strain sensing properties of the resultant fibres. This work addresses these key issues by developing a facile, efficient, and versatile wet-spinning method for the production of elastomeric conductive composite fibres. This platform has enabled the comparison of the properties of the composite fibres from three different types of organic conductors. The effects of the filler type (spherical, rod-like, and platelet) and filler loading on the electrical and mechanical properties of the resultant composite fibres were studied. This work provides practical insights on how the spinning platform, the conductive filler type, and loading levels influence the resultant mechanical and electrical properties of the conductive elastomeric fibres, as well as the strain sensing performance of the composite fibres.

## 2. Experimental

### 2.1. Materials

Polycarbonate-based thermoplastic PU (AdvanSource Biomaterials Chronoflex<sup>®</sup> C 80A), CB (VULCAN<sup>®</sup> XC72R, Lot No. GP-3919), SWCNTs (HiPco<sup>®</sup>, Continental Carbon, Lot No. P1001), *N,N*-dimethylformamide (DMF, Sigma-Aldrich), 1-cyclohexyl-2-pyrrolidone (CHP, Sigma-Aldrich), and isopropanol (Chem-Supply) were used without further purification.

### 2.2. Preparation of spinning formulations

The composite formulations for fibre spinning were prepared by making homogenous solvent-based dispersions of the filler, and then dissolving into them the required amount of PU pellets. For PU/CB, the CB was first dispersed in DMF at a concentration of 5 mg ml<sup>-1</sup> with the aid of probe sonication (Branson digital sonifier S-450D, 400 W, equipped with a 1/2" disruptor horn and a 1/8" microtip) at 30% amplitude for 60 min before the addition of PU pellets. For PU/SWCNT, the SWCNT was first dispersed in CHP at a concentration of 0.5 mg ml<sup>-1</sup> by probe sonication at 30% amplitude for 30 min before the addition of PU pellets. For PU/chemically converted graphene (CCG), CCG was synthesized using the previously described method [28, 29]. PU was dissolved at different concentrations in the CCG dispersion (in DMF) and were sonicated for 30 min prior to fibre spinning.

### 2.3. Fibre wet-spinning

PU/CB, PU/SWCNT and PU/CCG fibres were prepared using a wet-spinning method [12, 14, 18, 30–37]. This involved injecting the spinning formulations into a non-solvent bath with a vertical tubing attached, both of which were filled with isopropanol (as the non-solvent). The spinneret was a 23 gauge needle (nozzle diameter ~0.34 μm). The spinning solution flow rate was controlled at 1–5 ml h<sup>-1</sup> using a syringe pump. The composite fibres were collected on a winder and dried in air for 24 h. Annealing was carried out in an oven (Binder E28) at 170 °C for 12 h in air.

### 2.4. Characterization

An optical microscope (Leica DM EP) was used for measuring the diameter of the fibres. Measurements were carried out using the built-in image analysis tool in the Leica application suite with a minimum of 10 measurements along the fibre length). Fibre cross-sections were studied using a field emission SEM (JEOL JSM-7500FA). Fibres were broken while immersed in liquid nitrogen (~30 s) and then sputter coated (EDWARDS Auto 306) with platinum (~10 nm). The electrical conductivity of the composite fibres was measured under laboratory humidity and temperature conditions using an in-house linear four-point probe cell with 230 μm probe spacing. A galvanostat (Princeton Applied Research 363) was used to apply currents (I) between the outer probes and the voltages (V) between the two inner probes were recorded

using a digital multimeter (Agilent 34401A). The electrical conductivities were calculated from the  $I$ - $V$  curves and reported based on more than ten measurements for each condition. The mechanical properties of the composite fibres were measured using a tensile testing instrument (Shimadzu EZ-L) with a 2 N load cell. At least ten samples were tested for each condition. Samples were prepared by attaching the fibres to paper frames (10 mm in aperture). Uniaxial tensile tests were carried out until failure of the fibres with a strain rate (crosshead speed) of  $10 \text{ mm min}^{-1}$  ( $100\% \text{ min}^{-1}$ ). Values for Young's modulus, yield stress (stress at 5% strain), elongation at break, and toughness were calculated from the data using a custom-coded program in MATLAB® computational software. Electromechanical tests were carried out using real-time monitoring of the resistance during the cyclic extension-relaxation mechanical tests on the fibres using a digital multimeter (Agilent 34410A). Copper tape was placed at each end of the fibre to establish the connection and to allow the resistance measurements. The test was carried out by cyclic stretching of the fibre (10 cycles) to an applied strain of 10% and releasing the fibre to return to its unstretched state (zero strain). The applied strain magnitude was increased incrementally (with 10% strain steps) and the test was continued until failure of the sample. The resistance data was captured every 0.05 s and recorded in a personal computer using an analogue to digital (A/D) interface.

### 3. Results

The PU composite fibres containing various fillers (CB, spherical; SWCNTs, rod-like; and CCG, platelet) at different loadings (up to 16.7 wt.%) were prepared using the established wet-spinning protocol and the set-up reported previously by our group [12, 14, 18, 30–35]. The preparation of spinnable formulations was developed for each filler type as described in the experimental section. Table S1 (supplementary data) summarizes the spinning formulations for each filler type. It can be noted from this table that the maximum SWCNT loading is 4.8 wt.%. Above this loading, the formulation was no longer spinnable. By contrast, significantly higher filler loadings were achieved for CB (16.7 wt.%) and CCG (12.5 wt.%). During fibre spinning, it was observed that each spinning formulation required different fibre spinning conditions (i.e. flow rate) to achieve continuous fibre lengths of more than 10 m with circular diameter. This is in agreement with previous reports that the coagulation rate of fibre formation is dependent upon the filler loading and the solvent/non-solvent system during wet-spinning [18, 35, 38]. In order to ensure that optimal fibre spinning conditions were used for each sample, the cross-section of each fibre was monitored for its circularity. It can be seen from figure 1 that the utilized fibre spinning conditions resulted in fibres that exhibited good circularity. This observation suggests that the spinning conditions used for each sample have enabled efficient extraction of the solvent from the spinning dope (i.e. sufficiently low coagulation rates were attained) and have prevented the formation of a thick 'skin' layer around the jet.

Despite this uniformity, it can be observed from the SEM images that the fibres have distinct differences in their morphologies. PU/CB fibres contain CB aggregates that were uniformly distributed within the fibre. The cross-section of PU/CCG and PU/SWCNT fibres did not have the same features and it was not possible to isolate and identify individual or aggregates of CCG or SWCNT. These results suggest that these two fillers were highly exfoliated in the solvents and remained exfoliated and dispersed well within the PU matrix. It also suggests that both fillers have very good interactions with PU.

The electrical conductivity of PU/CB, PU/SWCNT, and PU/CCG fibres with various loadings were measured to elucidate the effects of filler type (spherical, rod-like, and platelet) and filler loading. Figure 2 shows the electrical conductivity of all samples. It can be seen that the lowest percolation threshold (i.e. the lowest onset of electrical conductivity) was obtained for PU/SWCNT fibre (rod-like filler) with 1.6 wt.% SWCNT loading. Fibres with lower SWCNT loadings did not exhibit electrical conductivity. The percolation thresholds of other PU composite fibres (with spherical or platelet fillers) were significantly higher than PU/SWCNT, which were obtained at 10.0 wt.% and 16.7 wt.% for PU/CCG and PU/CB fibres, respectively. For all fibres, the electrical conductivity increased with filler loading. The highest electrical conductivity of  $\sim 1.4 \text{ S m}^{-1}$  was obtained for PU/CB fibre, albeit at a very high CB loading of 16.7 wt.%. However, when the conductivity was normalized to filler content in terms of weight percent (figure S1(a)) and volume fraction (figure S1(b)), the PU/SWCNT fibres exhibited the highest conductivities even at the significantly lowest filler loadings compared to the PU/CB and PU/CCG fibres.

Uniaxial tensile stress-strain tests were carried out on the various PU composite fibres to identify the effects of filler type and filler loading on the degree of reinforcements and their mechanical behaviour. Figure 3 shows representative stress-strain curves for pure PU and for the PU composite fibres. Other fibres tested with the same composition exhibited very similar stress-strain behaviours. It was first noted that there were only minor variations in the stress-strain curves for pure PU fibres (figure S2(a)) which were reflective of the different solvents used in spinning formulations (DMF for PU/CB and PU/CCG fibres and CHP for PU/SWCNT fibres). Nevertheless, the pure PU fibres exhibited stress-strain behaviours that are typical for elastomers [39–41]. This behaviour is exemplified by the three distinct regions (figure S2(b)) that have been identified as follows: 1) the initial stiff response and yield (low strain, region I); 2) the strain-induced softening plateau region (medium strain, region II), and 3) the strain-induced hardening or crystallization region (high strain, region III). It was observed that the shape of the stress-strain curves for the composite fibres differed from that of the pure PU fibres. For example, the composite fibres displayed higher stresses in both the low and medium strain regions. This upward shift to a higher stress increased with filler loading for all PU composite fibres. The effects of filler loading on the properties in the high strain region varied significantly with filler type and loading.

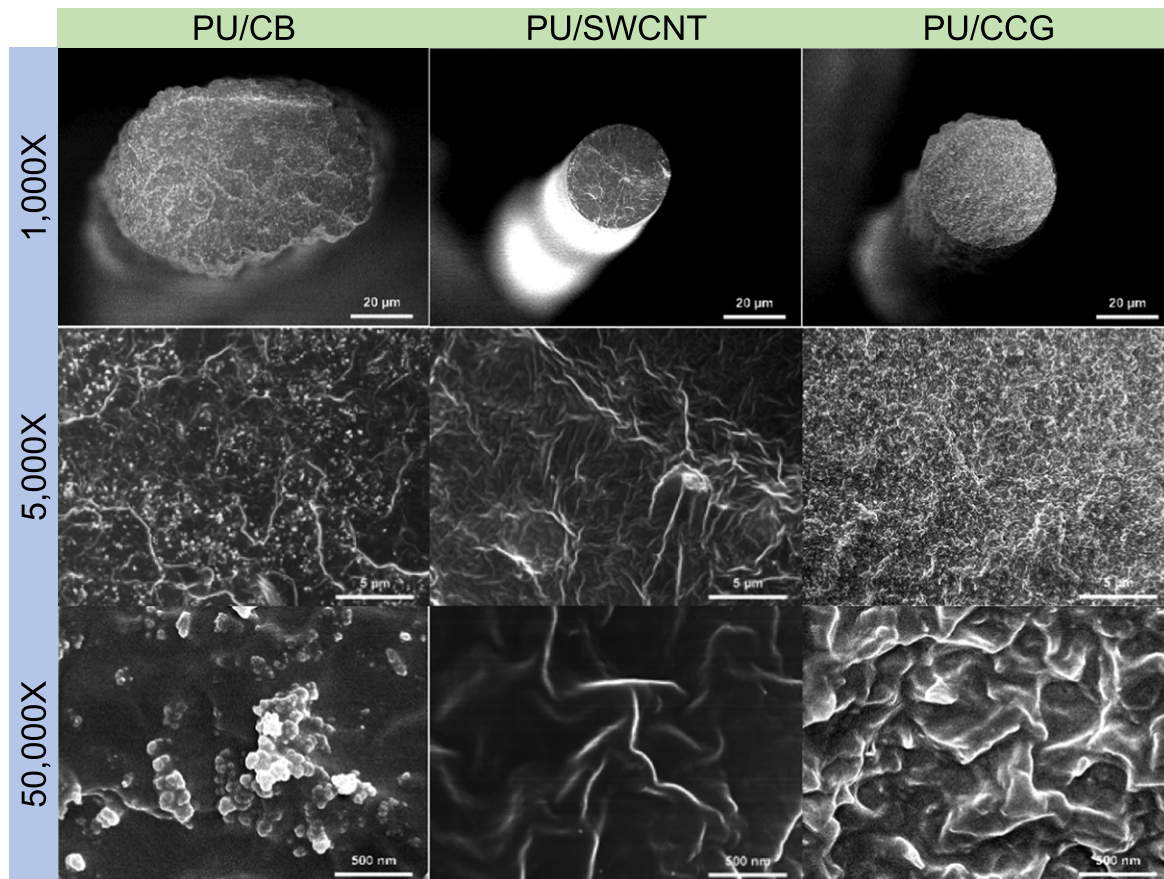


**Figure 1.** SEM images of the wet-spun PU/CB (16.7 wt.% CB), PU/SWCNT (4.8 wt.% SWCNT), and PU/CCG (12.5 wt.% CCG) composite fibres at different magnifications showing the circular cross-section morphology and homogeneous dispersion of the fillers.

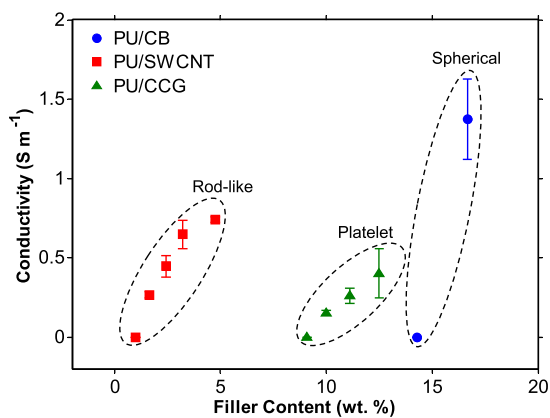


**Figure 2.** Electrical conductivity of the PU composite fibres at different loadings.

To differentiate the effects of filler type and loading in PU composite fibres, the stress–strain curves were analysed to quantify the values of Young's modulus ( $E$ ), yield stress (stress at 5% strain,  $\sigma_y$ ), tensile strength ( $\sigma$ ), elongation at break ( $\epsilon$ ), and toughness ( $T$ ). It was found that both  $E$  (figure 4(a)) and  $\sigma_y$  (figure 4(b)) increased with filler loading for all PU composite fibres, albeit at varying degrees. The highest increase in  $E$  (50 times higher than pure PU) and  $\sigma_y$  (28 times higher than pure PU) was observed for PU/SWCNT at the

maximum loading (4.8 wt.%). It was also noted that the use of CCG resulted in significantly lower  $E$  and required much higher loading for similar reinforcement in  $E$  and  $\sigma_y$  compared to PU/SWCNT. Very low enhancements of  $E$  and  $\sigma_y$  were achieved when CB was used as the filler. In terms of tensile strength ( $\sigma$ , figure 4(c)), an initial increase in  $\sigma$  with filler loading was observed for all PU composite fibres up to a filler loading of  $\sim 6$  wt.%. After this loading,  $\sigma$  decreased slightly with filler loading. Nevertheless, all composite fibres showed significant enhancement in tensile strength with the highest  $\sigma$  observed for PU/CCG fibres, which was  $\sim 60\%$  higher than the pure PU. When  $\sigma$  was normalized to filler loading, all composite fibres exhibited similar behaviour indicating that  $\sigma$  of the PU composite fibres was significantly affected by filler loading but not by filler type (figure S3).

The elongation at break ( $\epsilon$ ) of all PU composite fibres decreased with filler loading (figure 4(d)). However, the rate and magnitude of decrease in  $\epsilon$  varied with filler type. For PU/SWCNT fibres, there was an initial significant drop in  $\epsilon$  compared to pure PU, while there was a gradual decrease for PU/CCG and even more gradual for PU/CB. At the highest filler loading, PU/CB showed the least damaging impact on  $\epsilon$ , achieving a very high  $\epsilon$  of  $\sim 295\%$  at CB loading of 16.7 wt.%. By comparison, PU/SWCNT and PU/CCG fibres only achieved  $\epsilon$  of  $\sim 119\%$  and  $56\%$  at the highest filler loadings of 4.8 and 12.5 wt.%, respectively.

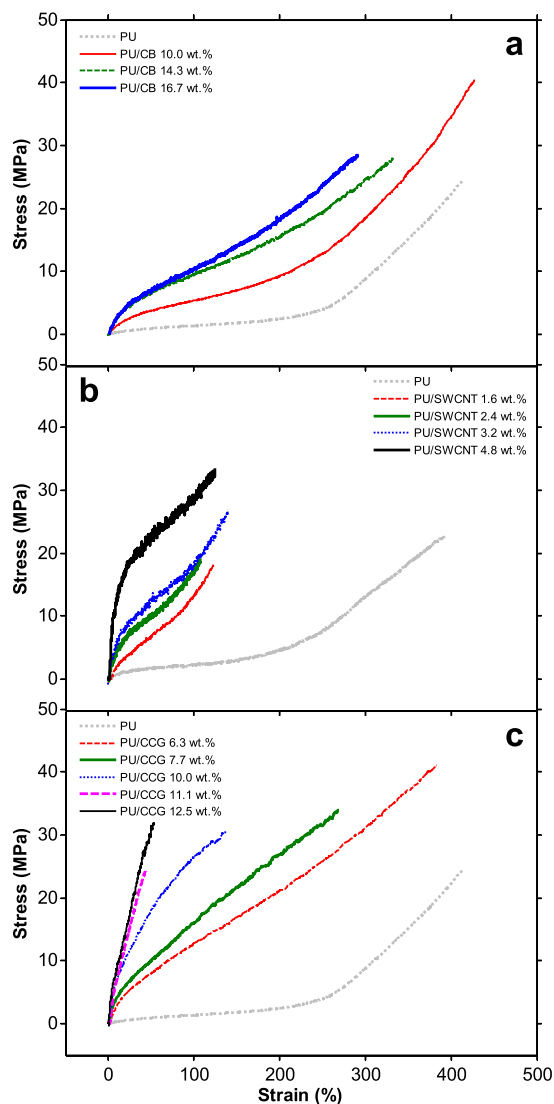


**Figure 3.** Representative stress–strain curves for (a) PU/CB, (b) PU/SWCNT, and (c) PU/CCG fibres.

In terms of toughness (figure 4(e)), it was observed that the effect of increasing the filler loading is different for PU/SWCNT compared to PU/CCG and PU/CB. Although the toughness of PU/SWCNT initially decreased compared to pure PU, it increased with subsequent increase in SWCNT loading. By contrast, PU/CCG and PU/CB initially showed an increase in toughness that decreased as filler loading was increased. The highest toughness of  $\sim 79.3 \text{ MJ m}^{-3}$  was achieved for PU/CCG at filler loading of 6.3 wt.%.

To evaluate the strain sensing properties of the various composite fibres, electromechanical cyclic tests were performed on selected samples. This test was carried out by monitoring the change in resistance during the extension–relaxation cycles. A sample for each composition was selected on the basis of elongation at break ( $>50\%$ ) and high electrical conductivity. The representative electromechanical results for each sample are shown in figure S4. From these data, strain sensing properties such as sensing range and

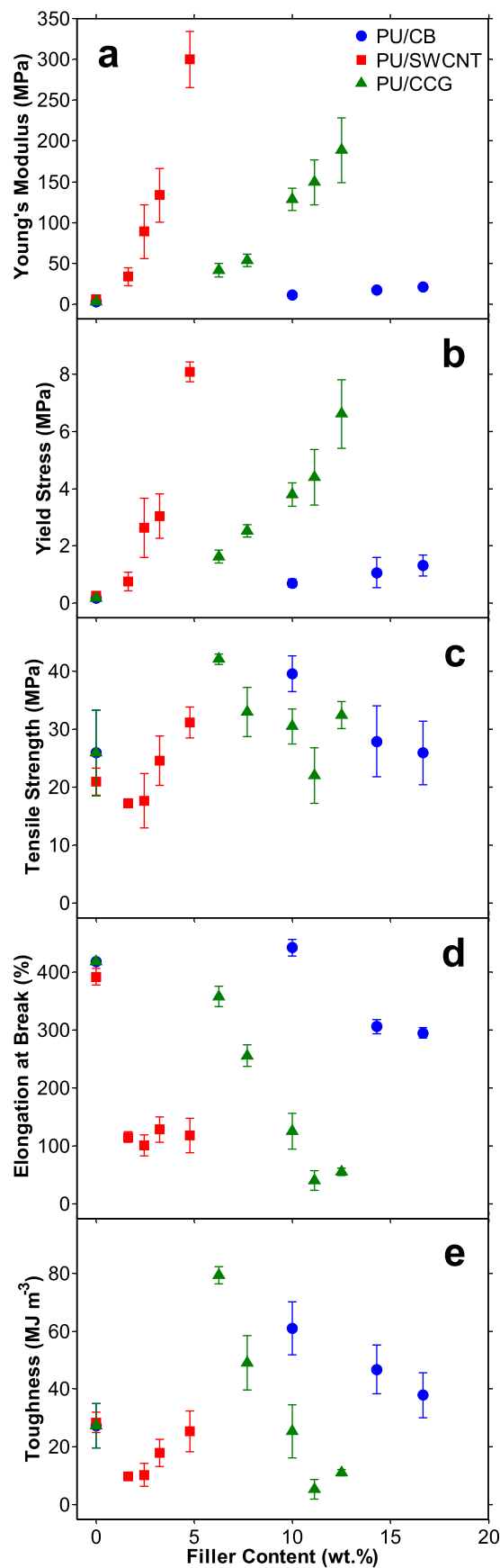


**Figure 4.** Mechanical properties of PU composite fibres: (a) Young’s modulus, (b) yield stress (stress at 5% strain), (c) tensile strength, (d) elongation at break, and (e) toughness.

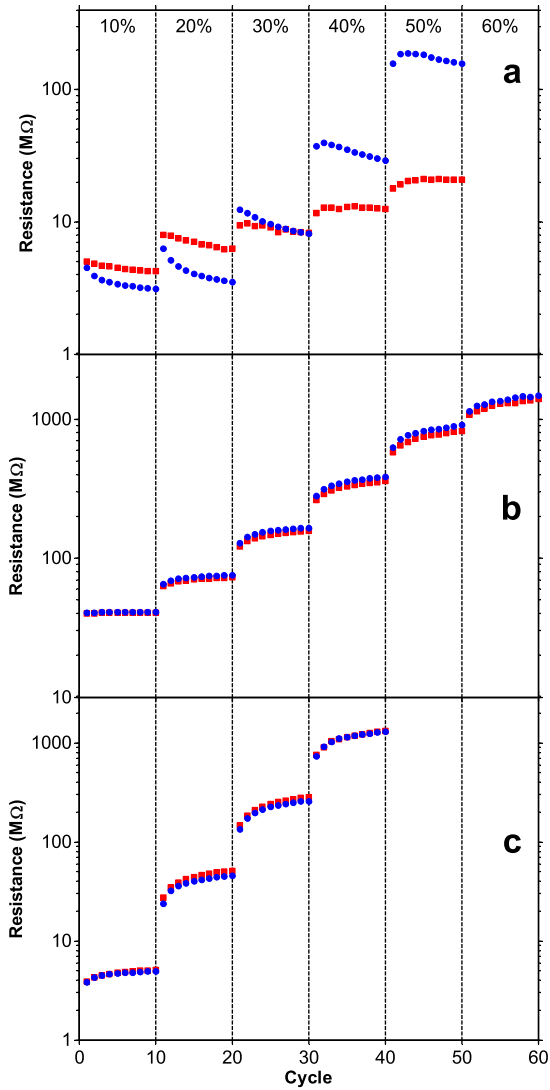


**Figure 5.** Strain sensing properties of PU composite fibres. Cyclic loading resistance (●) and unloading resistance (■) for the electromechanical test on: (a) PU/CB, (b) PU/SWCNT, and (c) PU/CCG fibres.

sensitivity were calculated. Figure 5 plots the loading resistance ( $R_{Loading}$ ) and unloading resistance ( $R_{Unloading}$ ) of the fibres during the electromechanical cyclic tests. The PU/SWCNT fibre exhibited the highest sensing range (up to 60% applied strain), followed by PU/CB (50%) and then PU/CCG (40%). At all applied strains, the resistance response of PU/SWCNT increased with stretching and decreased with relaxing (i.e.  $R_{Loading} > R_{Unloading}$ ). By contrast, PU/CCG and PU/CB revealed mixed strain sensing behaviours. In the case of PU/CB fibre, the cyclic  $R_{Loading}$  was lower than  $R_{Unloading}$  for up to 20% applied strain. This behaviour was reversed above 30% applied strain and the difference between  $R_{Loading}$  and  $R_{Unloading}$  increased significantly. For PU/CCG, the reversal was observed at 30% applied strain and the difference in resistance ( $R_{Loading} - R_{Unloading}$ ) was maintained.

The gauge factors ( $GF$ ) of the composite fibres were calculated at different stretching cycles.  $GF$  gives an

indication of the sensitivity and stability of the sensors at each applied strain cycle.  $GF$  is calculated based on the resistance of the fibres at the unstretched ( $R_0$ ), loading ( $R_{Loading}$ ), and unloading ( $R_{Unloading}$ ) states for each applied strain ( $\varepsilon$ ) using equation (1).

$$GF = \frac{R_{Loading} - R_{Unloading}}{\varepsilon R_0} \times 100. \quad (1)$$

PU/SWCNT and PU/CB displayed a stable sensing response at strain magnitudes of up to 40% for which the  $GF$  values remained linear within different cycles of each applied strain (figure S5). In agreement with the above observations on the mixed sensing behaviour of the PU/CB and PU/CCG fibres, the sign of  $GF$  changed for these fibres from negative to positive with increasing applied strain. These results show that PU/SWCNT fibre has the most consistent strain sensing behaviour (i.e. positive gauge factor at all applied strains with minimal variations).

#### 4. Discussion

The addition of different filler types to PU has affected the properties of the resulting composite formulations. This effect was demonstrated by the loading required for the high aspect ratio filler (SWCNTs  $\sim 10^3$ , length  $\sim 0.8$ – $1.2 \mu\text{m}$ ) [42], which was significantly lower than the low aspect ratio fillers (CB  $\sim 1$ , particle size 20–50 nm [43, 44], and CCG  $\sim 300$ , lateral size  $\sim 300$ – $400$  nm) [28, 29]. These changes have flow-on effects in achieving enhancements in electrical conductivity and mechanical properties. It was found that the aggregation of fillers in the PU/filler formulation was detrimental to electrical conductivity. For example, CB spherical particles were highly aggregated in the PU/CB fibres and exhibited a high percolation threshold for electrical conductivity. This result was consistent with previous reports on CB-filled elastomers [45, 46]. In contrast, composite fibres prepared from rod-like SWCNT and platelet CCG fillers, which were observed to be homogeneously dispersed within the PU matrix, have lower percolation thresholds. It is also likely that SWCNTs became orientated along the fibre axis during spinning, similar to previous reports [47, 48], which led to efficient filler contact and network formation resulting in enhanced electrical conductivity and mechanical reinforcement. The lower electrical properties and mechanical reinforcement of CCG than SWCNTs can be attributed to the inefficient interlocking and contact of the sheets in forming filler networks [49, 50].

The results in this study also highlight how each filler type influences the filler concentration dependent properties of the composite fibres. In terms of Young's modulus ( $E$ ) reinforcement, the data was analysed using the Voigt [51] model for the rule of mixture (equation (2)) because the fillers are much stiffer than PU

$$E = (\eta E_f - E_p)\phi + E_p. \quad (2)$$

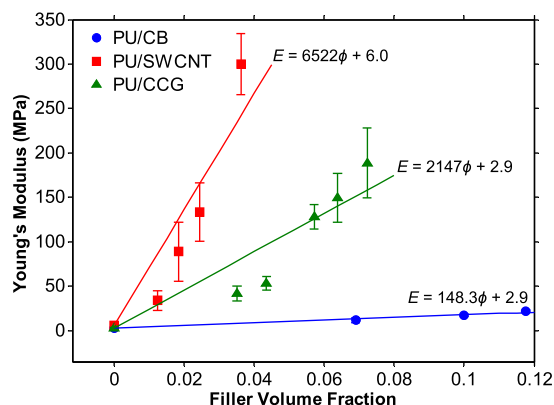


**Figure 6.** Reinforcement effect of fillers in PU composite fibres (the linear lines represent the best fit obtained by the Voigt model).

In this equation,  $E$ ,  $E_f$  and  $E_p$  are Young's moduli of the composite, the filler, and the polymer, respectively.  $\phi$  is the volume fraction of the filler and  $\eta$  is the filler efficiency factor.  $\phi$  was calculated based on the following density values:  $1.2 \text{ g cm}^{-3}$  for PU [52],  $1.8 \text{ g cm}^{-3}$  for CB [53],  $1.6 \text{ g cm}^{-3}$  for SWCNT [54], and  $2.2 \text{ g cm}^{-3}$  for CCG [55]. By fitting the  $E$  data for each composite fibre using equation (2) (figure 6), it was found that the slope ( $dE/d\phi$ , referred to as the rate of reinforcement) is significantly higher for PU/SWCNT (6.52 GPa) than for PU/CCG (2.15 GPa) and PU/CB (0.15 GPa) fibres. The  $dE/d\phi$  for PU/SWCNT fibres is also higher than those of previously reported values for filled elastomers (table S2). These results clearly show that reinforcement rates reflect the differences in the aspect ratios of the fillers. The highly debundled/exfoliated states of SWCNTs and CCG promoted PU–filler interactions that are much stronger than the interaction of aggregated and small aspect ratio CB with PU. These results are consistent with previous reports where high aspect ratio fillers were found to enhance the filler–PU interactions [3, 4, 56, 57]. The higher  $dE/d\phi$  for PU/SWCNT could also be the result of the formation of a more effective reinforcing filler network [58, 59], with better interlocking of the filler particles and PU soft segment chains as well as very little damage to the PU hard segment domains with filler addition [60, 61] as reported previously.

In the case of reinforcement in tensile strength ( $\sigma$ ), previous reports on PU composites have shown that good filler–PU interactions enhance  $\sigma$ , while the interruption in strain-induced crystallization of the soft segment phase and the disruption in hard segment domains both decrease  $\sigma$  [60, 61]. The results in this study suggest that the PU–filler interactions are effective only at low filler loadings, i.e. within the loading range used for SWCNTs. The significantly higher loading range used for both CCG and CB suggest detrimental effects on soft segment crystallization and hard segment domains. It can be deduced that high aspect ratio filler can enhance  $\sigma$  at low loading. Also, at high filler loading,  $\sigma$  is independent of the type of filler.

It has been shown that the inclusion of fillers in the PU soft segment phase interlocks the fillers and the PU chains in

this phase [62]. This interlocking is generally reflected in the increase in slope of the medium strain region of the stress–strain curves (region II, figure S2(b)), as seen in the PU composite fibres (figure 3). Very high interlocking levels, however, impede the extensibility of the soft segment phase resulting in low elongation at break ( $\epsilon$ ) [60, 61]. Fibre composites with SWCNT fillers resulted in a significant and abrupt decrease in  $\epsilon$  even at low loading, while CB resulted only in a slow and marginal decrease even when the loading was much higher than the SWCNT. It can therefore be deduced that the interlocking of soft PU chains was dependent upon filler aspect ratio such that the spherical fillers have the least damaging impact on  $\epsilon$ . This is further supported by the observed similar decrease in  $\epsilon$  with CCG but with much higher loading than SWCNTs.

The combinations of the improved stiffness, favourable interactions for increased strength, and low interruption of strain-induced crystallization and hard segment domains were manifested in the toughness ( $T$ ) of the composite fibres. The strong dependence of  $T$  on the filler type is similar to the trends observed for  $\epsilon$ , where spherical CB and rod-like SWCNT resulted in the highest and lowest  $T$ , respectively.

The ability to impart electrical conductivity to elastomers while maintaining or enhancing their mechanical properties provide the opportunity to expand their applications in strain sensing. It has been shown through electromechanical cyclic tests that the PU composite fibres respond to stretching by the change in electrical resistance. For each composite fibre combination, the composition with the highest conductivity and elongation at break of more than 60% were selected on the basis that body movements typically apply strains of up to  $\sim 55\%$  [23].

The mechanisms for the observed strain sensing behaviours (i.e. increasing or decreasing resistance with stretching, and *vice versa*) have been previously attributed to the rearrangement of fillers and the re-structuring of conducting networks [18]. When the conducting networks break during stretching, it is likely to result in resistance increase. Stretching, however, can also align filler particles and give rise to the formation of new conducting networks, thereby decreasing resistance [63]. The differences in strain sensing behaviours of the PU composite fibres can be attributed to the differences in the aspect ratio of the conducting fillers. In the case of PU/CB and PU/CCG fibres, during the first cycle, the initial increase in resistance is likely due to the loss of conduction paths from the breakage of the network of highly aggregated CB particles or CCG sheets. In the succeeding cycles, the mechanism for strain sensing may be driven by the alignment of the conducting fillers (having low deformation). The alignment of CB or CCG during stretching allows for the new conduction paths or networks to be created, which decrease the resistance. Further stretching, however, results in the separation of the conducting fillers and increases the resistance. In PU/SWCNT fibres, the high aspect ratio is likely to result in filler alignment during fibre spinning. The separation of the conducting fillers during stretching can decrease the number of conduction paths thereby increasing the resistance.



## 5. Conclusions

Electrically conductive elastomer composite fibres were successfully prepared using wet-spinning with various filler types and loadings. The analysis of the electrical and mechanical properties of the composite fibres revealed notable dependence on filler type, i.e. spherical CB, rod-like SWCNT, and platelet CCG as well as filler loading. The rod-like filler resulted in a significantly lower percolation threshold ( $\sim 1.6$  wt.%) and higher normalized conductivity than the spherical and platelet fillers (percolation threshold  $\geq 10$  wt.%). The Young's modulus and yield stress of the fibres increased with filler loading at varying degrees for different fillers, whereby the high aspect ratio SWCNT resulted in the highest enhancement in low strain tensile properties. The tensile strength of the fibres revealed strong dependence on filler loading and was found to be independent of filler type. The stretchability of the composites displayed dependence on the filler aspect ratio with the spherical CB having the least damaging impact on elongation at break. In terms of strain sensing properties, the resistance response of PU/SWCNT fibres increased with stretching and decreased with relaxing at all applied strains (i.e. the gauge factor values remained positive at all times). By contrast, the PU/CCG and PU/CB fibres exhibited mixed strain sensing behaviours (i.e. the gauge factor changed signs with applied strain). The largest sensing range was observed for the PU/SWCNT fibre (up to 60%), followed by PU/CB (50%) and then PU/CCG (40%). These results reveal the sensing strain range where each fibre type would most suitable for practical applications. The next research challenge is to evaluate whether these fibres can be developed into strain sensor textiles (and the evaluation of how they perform) for wearable strain sensing applications such as body movement measurement, medical monitoring, and sports injury prevention.

## Acknowledgments

The authors gratefully acknowledge financial support from the Australian Research Council (GGW and PCI on CE140100012, GGW on FL110100196 and JMR on FT130100380), the provision of facilities at the Australian National Fabrication Facility (Materials Node) and at the University of Wollongong Electron Microscopy Centre. We also thank Dr Sanjeev Gambhir for the synthesis of chemically converted graphene and the technical assistance of Drs Sina Naficy and Rouhollah Jalili.

## References

- [1] Gangopadhyay R and De A 2000 Conducting polymer nanocomposites: a brief overview *Chem. Mater.* **12** 608–22
- [2] Huang J-C 2002 Carbon black filled conducting polymers and polymer blends *Adv. Polym. Technol.* **21** 299–313
- [3] Coleman J N, Khan U, Blau W and Gunko Y 2006 Small but strong: a review of the mechanical properties of carbon nanotube-polymer composites *Carbon* **44** 1624–52
- [4] Kim H, Abdala A A and Macosko C W 2010 Graphene/polymer nanocomposites *Macromolecules* **43** 6515–30
- [5] Rogers J A, Someya T and Huang Y 2010 Materials and mechanics for stretchable electronics *Science* **327** 1603–7
- [6] Park M, Park J and Jeong U 2014 Design of conductive composite elastomers for stretchable electronics *Nano Today* **9** 244–60
- [7] Yan C and Lee P S 2014 Stretchable energy storage and conversion devices *Small* **10** 3443–60
- [8] Li C, Thostenson E T and Chou T-W 2008 Sensors and actuators based on carbon nanotubes and their composites: a review *Compos. Sci. Technol.* **68** 1227–49
- [9] Kong L and Chen W 2014 Carbon nanotube and graphene-based bioinspired electrochemical actuators *Adv. Mater.* **26** 1025–43
- [10] Hansen T S, West K, Hassager O and Larsen N B 2007 Highly stretchable and conductive polymer material made from poly(3,4-ethylenedioxythiophene) and polyurethane elastomers *Adv. Funct. Mater.* **17** 3069–73
- [11] Mattmann C, Clemens F and Tröster G 2008 Sensor for measuring strain in textile *Sensors* **8** 3719–32
- [12] Granero A J, Razal J M, Wallace G G and in het Panhuis M 2010 Elastic conducting carbon nanotube-laden SIBS fibers *2010 Int. Conf. on Nanoscience and Nanotechnology* (Sydney: IEEE) pp 80–3
- [13] Bilotti E, Zhang R, Deng H, Baxendale M and Peijs T 2010 Fabrication and property prediction of conductive and strain sensing TPU/CNT nanocomposite fibres *J. Mater. Chem.* **20** 9449–55
- [14] Granero A J, Wagner P, Wagner K, Razal J M, Wallace G G and in het Panhuis M 2011 Highly stretchable conducting SIBS-P3HT fibers *Adv. Funct. Mater.* **21** 955–62
- [15] Fan Q, Zhang X and Qin Z 2012 Preparation of polyaniline/polyurethane fibers and their piezoresistive property *J. Macromol. Sci. Part B* **51** 736–46
- [16] Tamburrano A, Sarasini F, De Bellis G, D'Aloia A G and Sarto M S 2013 The piezoresistive effect in graphene-based polymeric composites *Nanotechnology* **24** 465702
- [17] Ponnamma D, Sadasivuni K K, Strankowski M, Guo Q and Thomas S 2013 Synergistic effect of multi walled carbon nanotubes and reduced graphene oxides in natural rubber for sensing application *Soft Matter* **9** 10343
- [18] Seyedin M Z, Razal J M, Innis P C and Wallace G G 2014 Strain-responsive polyurethane/PEDOT:PSS elastomeric composite fibers with high electrical conductivity *Adv. Funct. Mater.* **24** 2957–66
- [19] Seyedin S, Razal J M, Innis P C, Jeiranikhameneh A, Beirne S and Wallace G G 2015 Knitted strain sensor textiles of highly conductive all-polymeric fibers *ACS Appl. Mater. Interfaces* **7** 21150–8
- [20] Thomassin J M, Jérôme C, Pardoën T, Bailly C, Huynen I and Detrembleur C 2013 Polymer/carbon based composites as electromagnetic interference (EMI) shielding materials *Mater. Sci. Eng. R Reports* **74** 211–32
- [21] Li Y, Cheng X Y, Leung M Y, Tsang J, Tao X M and Yuen M C W 2005 A flexible strain sensor from polypyrrole-coated fabrics *Synth. Met.* **155** 89–94
- [22] Wu J, Zhou D, Too C O and Wallace G G 2005 Conducting polymer coated lycra *Synth. Met.* **155** 698–701
- [23] Yamada T, Hayamizu Y, Yamamoto Y, Yomogida Y, Izadi-Najafabadi A, Futaba D N and Hata K 2011 A stretchable carbon nanotube strain sensor for human-motion detection *Nat. Nanotechnol.* **6** 296–301
- [24] Wang Y, Wang L, Yang T, Li X, Zang X, Zhu M, Wang K, Wu D and Zhu H 2014 Wearable and highly sensitive

- graphene strain sensors for human motion monitoring *Adv. Funct. Mater.* **24** 4666–70
- [25] Carpi F, DeRossi D and De Rossi D 2005 Electroactive polymer-based devices for e-textiles in biomedicine *IEEE Trans. Inf. Technol. Biomed.* **9** 295–318
- [26] Lymberis A and Olsson S 2003 Intelligent biomedical clothing for personal health and disease management: state of the art and future vision *Telemed. J. e-Health* **9** 379–86
- [27] Gibbs P T and Asada H H 2005 Wearable conductive fiber sensors for multi-axis human joint angle measurements *J. Neuroeng. Rehabil.* **2** 7
- [28] Li D, Müller M B, Gilje S, Kaner R B and Wallace G G 2008 Processable aqueous dispersions of graphene nanosheets *Nat. Nanotechnol.* **3** 101–5
- [29] Gambhir S, Murray E, Sayyar S, Wallace G G and Officer D L 2014 Anhydrous organic dispersions of highly reduced chemically converted graphene *Carbon* **76** 368–77
- [30] Jalili R, Aboutalebi S H, Esrafilzadeh D, Shepherd R L, Chen J, Aminorroaya-Yamini S, Konstantinov K, Minett A I, Razal J M and Wallace G G 2013 Scalable one-step wet-spinning of graphene fibers and yarns from liquid crystalline dispersions of graphene oxide: towards multifunctional textiles *Adv. Funct. Mater.* **23** 5345–54
- [31] Aboutalebi S H et al 2014 High-performance multifunctional graphene yarns: toward wearable all-carbon energy storage textiles *ACS Nano* **8** 2456–66
- [32] Jalili R, Razal J M, Innis P C and Wallace G G 2011 One-step wet-spinning process of poly(3,4-ethylenedioxythiophene): poly(styrenesulfonate) fibers and the origin of higher electrical conductivity *Adv. Funct. Mater.* **21** 3363–70
- [33] Jalili R, Razal J M and Wallace G G 2012 Exploiting high quality PEDOT:PSS–SWNT composite formulations for wet-spinning multifunctional fibers *J. Mater. Chem.* **22** 25174
- [34] Jalili R, Razal J M and Wallace G G 2013 Wet-spinning of PEDOT:PSS/functionalized-SWNTs composite: a facile route toward production of strong and highly conducting multifunctional fibers *Sci. Rep.* **3** 3438
- [35] Seyedin M Z, Razal J M, Innis P C, Jalili R and Wallace G G 2015 Achieving outstanding mechanical performance in reinforced elastomeric composite fibers using large sheets of graphene oxide *Adv. Funct. Mater.* **25** 94–104
- [36] Seyedin S, Romano M S, Minett A I and Razal J M 2015 Towards the knittability of graphene oxide fibres *Sci. Rep.* **5** 14946
- [37] Seyedin S, Razal J M, Innis P C, Jalili R and Wallace G G 2016 Compositional effects of large graphene oxide sheets on the spinnability and properties of polyurethane composite fibers *Adv. Mater. Interfaces* (doi:10.1002/admi.201500672)
- [38] Ziabicki A 1976 *Fundamentals of Fibre Formation: The Science of Fibre Spinning and Drawing* (London: Wiley)
- [39] Christenson E M, Anderson J M, Hiltner A and Baer E 2005 Relationship between nanoscale deformation processes and elastic behavior of polyurethane elastomers *Polymer* **46** 11744–54
- [40] Yeh F, Hsiao B S, Sauer B B, Michel S and Siesler H W 2003 *In-situ* studies of structure development during deformation of a segmented poly(urethane–urea) elastomer *Macromolecules* **36** 1940–54
- [41] Petrović Z S and Ferguson J 1991 Polyurethane elastomers *Prog. Polym. Sci.* **16** 695–836
- [42] Bergin S D, Sun Z, Streich P, Hamilton J and Coleman J N 2010 New solvents for nanotubes: approaching the dispersibility of surfactants *J. Phys. Chem. C* **114** 231–7
- [43] Donnet J-B, Bansal R C and Wang M-J 1993 *Carbon Black* (New York: CRC Press)
- [44] Liang J, Qiao S Z, Qing G and Lu M 2012 *Novel Carbon Adsorbents* ed J M D Tascón (Oxford: Elsevier Ltd) pp 549–81
- [45] Pantea D, Darmstadt H, Kaliaguine S and Roy C 2003 Electrical conductivity of conductive carbon blacks: influence of surface chemistry and topology *Appl. Surf. Sci.* **217** 181–93
- [46] Jha V, Thomas A, Bennett M and Busfield J 2010 Reversible electrical behavior with strain for a carbon black-filled rubber *J. Appl. Polym. Sci.* **116** 541–6
- [47] Blighe F M, Young K, Vilatela J J, Windle A H, Kinloch I A, Deng L, Young R J and Coleman J N 2011 The effect of nanotube content and orientation on the mechanical properties of polymer-nanotube composite fibers: separating intrinsic reinforcement from orientational effects *Adv. Funct. Mater.* **21** 364–71
- [48] Khan U, Young K, O'Neill A and Coleman J N 2012 High strength composite fibres from polyester filled with nanotubes and graphene *J. Mater. Chem.* **22** 12907
- [49] Du J, Zhao L, Zeng Y, Zhang L, Li F, Liu P and Liu C 2011 Comparison of electrical properties between multi-walled carbon nanotube and graphene nanosheet/high density polyethylene composites with a segregated network structure *Carbon* **49** 1094–100
- [50] Martin-Gallego M, Bernal M M, Hernandez M, Verdejo R and Lopez-Manchado M A 2013 Comparison of filler percolation and mechanical properties in graphene and carbon nanotubes filled epoxy nanocomposites *Eur. Polym. J.* **49** 1347–53
- [51] Voigt W 1889 Über die Beziehung zwischen den beiden Elastizitätskonstanten isotroper Körper *Wied. Ann.* **38** 573–87
- [52] AdvanSource Biomaterials 2011 *ChronoFlex C® Factsheet*
- [53] Cabot Corporation 2015 *Cabot VULCAN® XC72 Datasheet*
- [54] Continental Carbon Nanotechnologies *HiPco® Single-Wall Carbon Nanotubes Datasheet*
- [55] May P, Khan U, O'Neill A and Coleman J N 2012 Approaching the theoretical limit for reinforcing polymers with graphene *J. Mater. Chem.* **22** 1278–82
- [56] Coleman J N, Khan U and Gun'ko Y K 2006 Mechanical reinforcement of polymers using carbon nanotubes *Adv. Mater.* **18** 689–706
- [57] Potts J R, Dreyer D R, Bielawski C W and Ruoff R S 2011 Graphene-based polymer nanocomposites *Polymer* **52** 5–25
- [58] Bokobza L 2007 Multiwall carbon nanotube elastomeric composites: a review *Polymer* **48** 4907–20
- [59] Fu S-Y, Feng X-Q, Lauke B and Mai Y-W 2008 Effects of particle size, particle/matrix interface adhesion and particle loading on mechanical properties of particulate–polymer composites *Compos. Part B Eng.* **39** 933–61
- [60] Liff S M, Kumar N and McKinley G H 2007 High-performance elastomeric nanocomposites via solvent-exchange processing *Nat. Mater.* **6** 76–83
- [61] Khan U, Blighe F M and Coleman J N 2010 Selective mechanical reinforcement of thermoplastic polyurethane by targeted insertion of functionalized SWCNTs *J. Phys. Chem. C* **114** 11401–8
- [62] Chatterjee S, Nafezarefi F, Tai N H, Schlagenhauf L, Nüesch F A and Chu B T T 2012 Size and synergy effects of nanofiller hybrids including graphene nanoplatelets and carbon nanotubes in mechanical properties of epoxy composites *Carbon* **50** 5380–6
- [63] Zhao H, Zhang Y, Bradford P D, Zhou Q, Jia Q, Yuan F-G and Zhu Y 2010 Carbon nanotube yarn strain sensors *Nanotechnology* **21** 305502–6